Essence of conservation forms in the traveling wave solutions of higher-order traffic flow models

Peng Zhang[1] and S. C. Wong[2,*]
[1]*Shanghai Institute of Applied Mathematics and Mechanics, Shanghai University, Shanghai, China*
[2]*Department of Civil Engineering, The University of Hong Kong, Hong Kong SAR, China*
(Received 1 April 2006; revised manuscript received 19 May 2006; published 9 August 2006)

This paper shows the essence of conservation forms when applying the weak solution theory to solve the traveling wave solution of a wide cluster in the Payne-Whitham (PW) model. The consideration of the conservation form for the acceleration equation is an important ingredient in the development of higher-order traffic flow models, but it is largely ignored in the research community. To fix the idea, we define two conservation forms for the same PW model, and consequently derive two solutions with different sets of characteristic parameters of the wide cluster. The analytical results are in good agreement with those that are obtained from numerical simulations. Moreover, these two solutions are also shown to be asymptotic to those of the well-known Kühne and Kerner-Konhaüser models with a viscosity term. More importantly, the careful treatment of the conservation form for the acceleration equation closes the important gap in the literature. Without the conservation form, the solution obtained depends very much on the design of numerical schemes, and can be quite arbitrary and may not adequately conform to the physically relevant properties.

DOI: 10.1103/PhysRevE.74.026109 PACS number(s): 89.40.Bb

I. INTRODUCTION

Macroscopic models have played important roles in describing many nonlinear complexities in traffic flow since the proposition of the Lighthill-Whitham-Richards (LWR) theory [1,2]. In this theory, vehicles on a highway as a whole are viewed as a continuum with a density ρ, an average v, and a flow $q=\rho v$, which are functions of location x and time t. From the conservation of mass as in fluid dynamics, the temporal change in density is related to the spatial change in flow rate such that

$$\frac{\partial \rho}{\partial t}+\frac{\partial \rho v}{\partial x}=0. \tag{1}$$

With a velocity-density relation $v=v_e(\rho)$, Eq. (1) becomes complete and constitutes the well-known LWR model. This model is fundamental for the study of hyperbolic waves and describes some basic nonlinear phenomena in traffic flow [3,4]. Recent attempts have also been made to extend the model to heterogeneous drivers [5–7].

To retrieve the dynamics in traffic, Payne [8] and Whitham [3] took acceleration into account. Together, these studies are known as the PW model. Other descriptions of the acceleration have followed, e.g., in [9–14]. The acceleration of all of these models takes a similar form as follows:

$$\frac{\partial v}{\partial t}+v\frac{\partial v}{\partial x}=\frac{v_e(\rho)-v}{\tau}-\frac{c_0^2(\rho)}{\rho}\frac{\partial \rho}{\partial x}+\nu\frac{\partial^2 v}{\partial x^2}, \tag{2}$$

which together with Eq. (1) constitutes the macroscopic traffic flow model. Here, the three terms on the right-hand side are related to physical forces of relaxation (or fluctuation), pressure, and viscosity, respectively, and $c_0(\rho)$ (>0) is the sound speed. If $\nu=0$, then the system is called a nonviscous model; otherwise, it is classified as a viscous model. The models that Kühne [9] and Kerner and Konhaüser (KK) [10,11] proposed belong to the class of viscous models with ν being a positive constant and $\nu=\mu/\rho$, where μ is a positive constant. In addition, Eq. (2) reduces to the PW model for $\nu=0$. For simplicity in our discussion, $c_0(\rho)$ is assumed to be a constant, i.e., $c_0(\rho)\equiv c_0$.

The most remarkable feature of the three aforementioned higher-order models (and probably some others) is their ability to reproduce stop-and-go waves. Such numerical examples were widely reported, such as in [10,15], adopting a non-convex equilibrium flow-density function $q_e(\rho)\equiv\rho v_e(\rho)$. These examples are typical of phase transitions between free, congested, and jam traffic states. In the transition, traffic dynamics is rich in hysteresis by which vehicular acceleration and deceleration paths are different in the phase diagram. For a wide cluster of stop-and-go waves, the phase plot can be represented by a straight line, which suggests that the structure of the cluster is a traveling wave solution. As important nonlinear complex phenomena, stop-and-go waves have been widely observed and reported through field studies [16,17]. Therefore, for the study of a higher-order model, it is theoretically significant to determine the parameters of the cluster, such as the maximal and minimal densities and the propagation speed.

However, the essence of the conservation form of an acceleration equation has not yet been well recognized in the traffic flow research community. This is probably because a "pressure" or "fluctuation" in traffic flow problems is merely a generalized force, and thus the conservation of "momentum" ρv is not required. Consequently, in many studies the velocity v or flow ρv was casually used as a solution variable without specific definition of a clear conservation form of the acceleration equation. In this paper, we emphasize that defining such a conservation form is essential because only so can the solution be uniquely determined in the presence of discontinuities. See [3,18–21] for detailed accounts of the related weak solution theory of hyperbolic conservation laws.

*Corresponding author. Email address: hhecwsc@hkucc.hku.hk

To show this essence in the present paper, we define two conservation forms of the PW model with v and ρv as the conservative variables, which are, respectively, called conservation form 1 (CF1) and conservation form 2 (CF2). In the context of the aforementioned wide cluster, we adopt the two conservation forms to indicate two different traveling wave solutions analytically, each with determined characteristic parameters. A cornerstone in each investigation is the application of the *Rankine-Hugoniot* conditions at the upstream front of the cluster, which proves to be a shock. We should mention that some algebraic equations of the parameters were also acquired in a recent study [15], but they were not sufficient to ensure a deterministic description because of the incomplete application of the *Rankine-Hugoniot* conditions. A relevant description can also be found in a recent report [22], in which the "anisotropic" traffic flow model Jiang *et al.* [23] proposed was adopted.

Defining the two conservation forms is also for the purpose of relating the PW model to the Kühne and KK models. Each of the two viscous models should also be written in a certain conservation form according to the viscosity term νv_{xx} or μv_{xx}. As the viscosity coefficient ν (or μ) vanishes, actually the Kühne (or KK) model possesses the same conservation form as CF1 (or CF2) of the PW model. This suggests that the former solution is asymptotic to that of the latter, according to the weak solution theory. Such relations are analogous to that between the inviscid and viscid Burgers' equations, or more generally that between hyperbolic conservation laws and their diffusive versions. See [3,19,20].

We note that the asymptotic theory can be applied to a viscous higher-order traffic flow model for solving the parameters of wide clusters. By the theory Kerner *et al.* [11] obtained the same algebraic equations as ours that are based on CF2. However, these parameters are merely "asymptotic" to the true values in the KK model with errors of the order $O(\mu)$, whereas they are exact in the PW model, corresponding to CF2. This is in accordance with the above arguments. When adopting the Kühne model and following similar discussion in [11] (or the references therein), it is expected to derive the same algebraic equations as ours that are based on CF1. Similarly, the resultant parameters are exact in the PW model, corresponding to CF1, whereas they are "asymptotic" to the true values in the Kühne model. Derivations of the referred algebraic equations from the asymptotic theory are expatiatory; they are not included in the forthcoming discussion.

Section II derives the characteristic parameters of a wide cluster in the PW model, in which many of the above arguments are highlighted. To support our conclusions, numerical simulation is implemented in Sec. III to generate clusters in their fully developed stage, namely for $t\to\infty$. As expected, these parameter values that are acquired from numerical examples agree very well with those that are derived analytically. In Sec. IV, we conclude the paper with several remarks.

II. DERIVATION OF CHARACTERISTIC PARAMETERS OF A WIDE CLUSTER

If $\nu=0$, then Eqs. (1) and (2) represent the PW model. For a flow function $q_e(\rho)=\rho v_e(\rho)$ that is concave for some lower density region but convex for the other, say with

$$v_e(\rho) = v_f\left\{\left[1+\exp\left(\frac{\rho/\rho_m - 0.25}{0.06}\right)\right]^{-1} - 3.72\times 10^{-6}\right\}, \tag{3}$$

we consider a traveling wave solution in this section. Here, v_f is the free flow velocity that is close to $v_e(0)$, ρ_m is the maximal density such that $v_e(\rho_m)$ is nearly zero [10,25], and the constants 0.25 and 0.06 are adjustable to empirical data. We note that adopting other nonconvex flow functions gives rise to similar properties.

We are now concerned with a traveling wave solution with propagation speed a (Fig. 1). For this we anticipate a wide cluster that is characterized by a jam $\rho=\rho_B$ and free flow $\rho=\rho_A$ in its surroundings. In Fig. 1(a) we assume that this solution consists of three constant flows with an upstream front and a downstream front in between. In Fig. 1(b), the aforementioned constant flows are assumed to be in equilibrium with $q_A=q_e(\rho_A)$ and $q_B=q_e(\rho_B)$, which are in the concave and convex parts of the fundamental diagram. Here, we refer to "a wide cluster" such that the constant region of $\rho=\rho_B$ in Fig. 1(a) is sufficiently long. This includes the limit case in which $\rho=\rho_B$ reduces to a single state. Referring to Fig. 1(a), we note that the cluster as a traveling wave solution can propagate with unchanged profile when assuming an initial or an initial and (periodic) boundary value problem and taking the whole profile as the initial state.

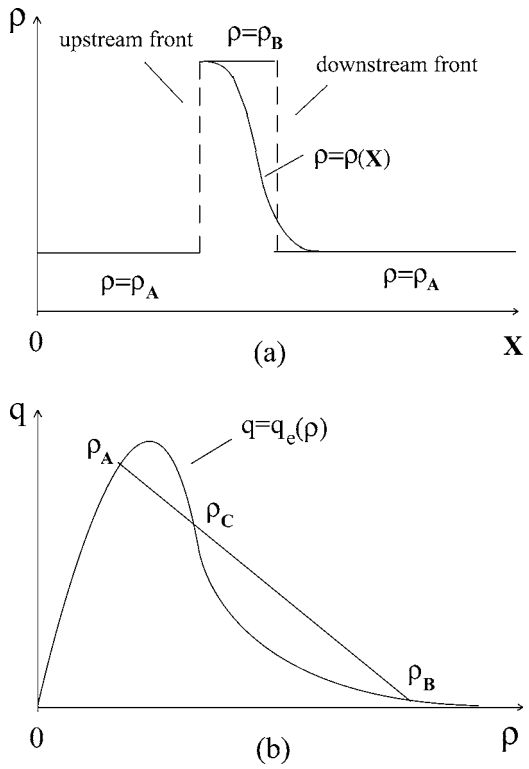

FIG. 1. Traveling wave solution with an upstream and a downstream front; (a) steady density distribution in the transformed coordinate; and (b) phase states (ρ,q) in comparison with the fundamental diagram $q=q_e(\rho)$.

A. Downstream front of the cluster

For a smooth piece (presumably the upstream or downstream front) that links two adjacent constant states, we make the transformation: $\rho(x,t)=\rho(X)$ and $v(x,t)=v(X)$, with $X=x-a$. Substituting these into Eqs. (1) and (2) leads to

$$\frac{d\rho}{dX}=\frac{q_e(\rho)-q}{\tau[c_0^2-(q_0/\rho)^2]}\equiv g(\rho),\quad q=a\rho+q_0, \tag{4}$$

where q_0 is an integral constant. See also [3] for a similar derivation in which a strictly concave function $q_e(\rho)$ was assumed. The second equation of Eq. (4) suggests that the phase diagram of the smooth solution piece corresponds to a segment of a straight line in the density-flow plane, which has a slope a. Suppose that the smooth piece connects the two constant flow states $[\rho_A,q_e(\rho_A)]$ and $[\rho_B,q_e(\rho_B)]$. The segment is then indicated as $\overline{AB}$ in Fig. 1(b) with slope $a<0$. Thus it is also implied by Eq. (4) that $q_0>0$.

We note that any smooth piece determined by the first equation of Eq. (4) is valid only if ρ is monotone of X. Otherwise, we would obtain multiple solutions of $\rho(X)$ in the inverse curve $X=\int^{\rho}[g(\rho)]^{-1}d\rho$. For this case, the two states should be separated by a shock, as will be described in the following section. For the smooth piece, we assume an equilibrium state (ρ_C,q_C), which is the intersection of segment $\overline{AB}$ and curve $q=q_e(\rho)$ [Fig. 1(b)]. The numerator of $g(\rho)$ in Eq. (4) then changes from a positive sign in $\rho_A<\rho<\rho_C$ to a negative sign in $\rho_C<\rho<\rho_B$. Therefore the denominator of $g(\rho)$ changes sign accordingly. This can be satisfied if and only if

$$\rho_C=\frac{q_0}{c_0},\quad \text{with } q_e(\rho_C)=a\rho_C+q_0, \tag{5}$$

by which the denominator of $g(\rho)$ changes from a negative sign in $\rho_A<\rho<\rho_C$ to a positive sign in $\rho_C<\rho<\rho_B$. This ensures that $d\rho/dX=g(\rho)<0$ in the set $(\rho_A,\rho_C)\cup(\rho_C,\rho_B)$. At the intersection C, $\rho=q_0/c_0$ must be a removable singularity of the function $g(\rho)$, and this is also ensured by Eq. (5) with

$$\left.\frac{d\rho}{dX}\right|_{\rho=\rho_C}=\lim_{\rho\to\rho_C}\frac{d\rho}{dX}=\lim_{\rho\to\rho_C}\frac{(q_e(\rho)-q)'}{\tau[c_0^2-(q_0/\rho)^2]'}$$
$$=\rho_C\frac{q_e'(\rho_C)-a}{2\tau c_0^2}<0,$$

where $q_e'(\rho_C)<a$ is self-evident through Fig. 1(b).

In summary, we can only have $d\rho/dX=g(\rho)<0$ for $\rho\in(\rho_A,\rho_B)$. With one parameter fixed, other parameters can be solved from the above equations. Given ρ_C, for example, q_0 and a can be solved explicitly from Eq. (5). Thus ρ_A and ρ_B can be solved as the intersections between the curve $q=q_e(\rho)$ and the segment $\overline{AB}$. Namely, we have

$$a=\frac{q_e(\rho_A)-q_e(\rho_B)}{\rho_A-\rho_B},\quad q_0=q_e(\rho_A)-a\rho_A,\quad \text{or} \tag{6}$$

$$q_0=q_e(\rho_B)-a\rho_B.$$

We note that the smooth connection between the discussed smooth piece and the constant flow $\rho=\rho_A$ (or $\rho=\rho_B$) is ensured by $d\rho/dX|_{\rho=\rho_A}=g(\rho_A)=0$ [or $d\rho/dX|_{\rho=\rho_B}=g(\rho_B)=0$]. Furthermore it is of much interest to derive from Eq. (5) that $a=v_e(\rho_C)-c_0$, which is also the first characteristic speed at the equilibrium state C. In other words, the propagation of the first characteristic at the transition synchronizes the traveling wave.

Obviously, the above discussion is suited only to the downstream front of the cluster considered, which links the upper region $\rho=\rho_B$ to the lower region $\rho=\rho_A$. For such a smooth piece, we note that a conservation form of the system is unnecessary because no discontinuity is involved. As there is one degree of freedom left for parameters ρ_A, ρ_B, and a, an additional equation is still needed for a deterministic description of the cluster. We therefore turn our attention to the upstream front.

B. Upstream front of the cluster

Smooth connection at the upstream front is impossible because of the aforementioned requirement that the density $\rho(X)$ must be monotonic decreasing. To avoid the problem being ill-posed, the requirement for smoothness has to be relaxed and a discontinuity must be introduced to separate the two constant flows $\rho=\rho_A$ and $\rho=\rho_B$. To determine this discontinuity, the model equations should be written in conservation forms.

Equation (1) is for the mass conservation with specific physical meanings, which means that it cannot be altered. However, the conservation for Eq. (2) is largely ignored in traffic flow problems. For the reasons that are mentioned in Sec. I, we define two conservation forms for Eq. (2). This means that we consider two systems of the PW model, the solutions of which are different if there is any discontinuity. First, we define the following:

CF1:

$$\frac{\partial v}{\partial t}+\frac{\partial}{\partial x}(0.5v^2+c_0^2\ln\rho)=\frac{v_e(\rho)-v}{\tau}. \tag{7}$$

Then, we view the "momentum" $q=\rho v$ to be conservative and thus define

CF2:

$$\frac{\partial q}{\partial t}+\frac{\partial}{\partial x}(q^2/\rho+c_0^2\rho)=\frac{q_e(\rho)-q}{\tau}. \tag{8}$$

We derive these forms from Eqs. (1) and (2) through differentiation.

Denote a general conservation system by the following:

$$\frac{\partial u}{\partial t}+\frac{\partial f(u)}{\partial x}=s(u). \tag{9}$$

Note that a system with source terms is also called balance laws. Assume that $\tau>\tau_0$ for some certain $\tau_0>0$. Thus source term $s(u)$ is smooth and bounded. With this assumption, we emphasize that the *Rankine-Hugoniot* conditions are appli-

cable to Eq. (9) and remain the same as those for the case of $s(u)=0$. We assume that two solution states, u_A and u_B, are separated by a discontinuity with wave speed a. Then the *Rankine-Hugoniot* conditions read:

$$f(u_A) - f(u_B) = a(u_A - u_B). \tag{10}$$

Note that the above vector form is applied component by component, and that a shock structure described by Eq. (10) also constitutes a traveling wave solution.

We set $u=(\rho,v)^T$, $f(u)=(\rho v, 0.5v^2+c_0^2 \ln \rho)$, and $s(u)=\{0,\tau^{-1}[v_e(\rho)-v]\}^T$, by which Eq. (9) stands for the system of Eqs. (1) and (7). Being relevant to the upstream front (Fig. 1), we substitute these into Eq. (10) to yield two equations; one coincides with the first equation of Eq. (6), and the other is arranged as the following:

CF1:

$$a = 0.5[v_e(\rho_A) + v_e(\rho_B)] + \frac{c_0^2 \ln \rho_A/\rho_B}{v_e(\rho_A) - v_e(\rho_B)}. \tag{11}$$

Equations (5), (6), and (11) together constitute the set of equations for the determination of the characteristic parameters of the cluster.

Setting $u=(\rho,q)^T$, $f(u)=(q,q^2/\rho+c_0^2\rho)^T$, and $s(u)=\{0,\tau^{-1}[q_e(\rho)-q]\}^T$, by which Eq. (9) stands for the system of Eqs. (1) and (8), we similarly obtain

CF2:

$$a = \frac{v_e^2(\rho_A)\rho_A - v_e^2(\rho_B)\rho_B}{q_e(\rho_A) - q_e(\rho_B)} + \frac{c_0^2(\rho_A - \rho_B)}{q_e(\rho_A) - q_e(\rho_B)}. \tag{12}$$

Equations (5), (6), and (12) are used to determine the parameters in the system of Eqs. (1) and (8).

It is evident that weak (discontinuous) solutions for CF1 and CF2 are different because Eqs. (11) and (12) are different. In other words, the system of Eqs. (1) and (7) is different from the system of Eqs. (1) and (8) in the sense of weak solution. See [3,18–21] for detailed accounts about the theory.

C. Characteristic parameters of the cluster

The parameters ρ_A, ρ_B, ρ_C, a, and q_0 can only be determined implicitly for each system. Precisely, these can be reduced to two unknowns with two equations. In the system of Eqs. (1) and (7), the two equations are acquired from Eqs. (5), (6), and (11), and can be arranged as follows:

CF1:

$$\frac{\rho_A\rho_B[v_e(\rho_A) - v_e(\rho_B)]}{\rho_C(\rho_B - \rho_A)} = v_e(\rho_C) - \frac{q_e(\rho_A) - q_e(\rho_A)}{\rho_A - \rho_B} = c_0, \tag{13}$$

where ρ_C is the density of the unique intermediate equilibrium state in the transition layer,

$$\rho_C = \rho_A\rho_B\sqrt{\frac{2\ln(\rho_A/\rho_B)}{\rho_B^2 - \rho_A^2}}.$$

In the system of Eqs. (1) and (8), an alternative form can similarly be obtained by Eqs. (5), (6), and (12),

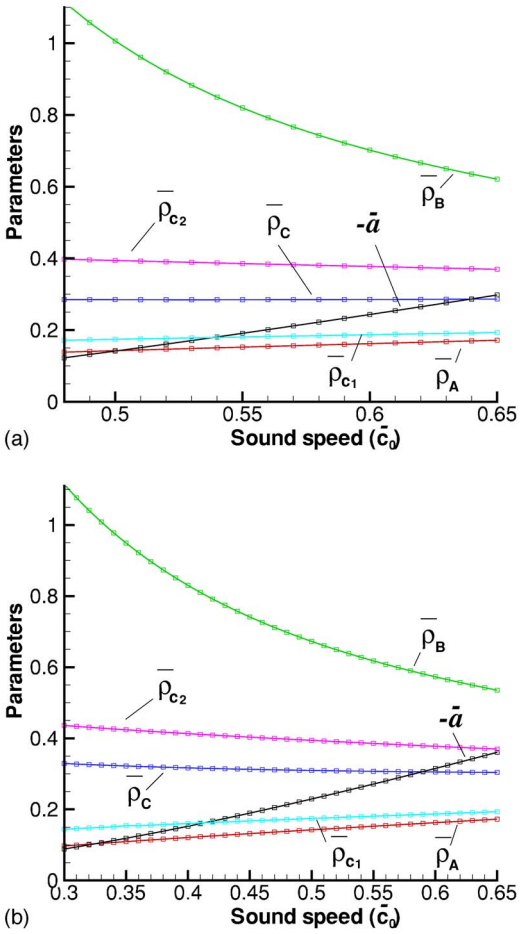

FIG. 2. (Color online) Dependency of characteristic parameters on the sound speed, illustrated as curves for a wide sound speed range. (a) For CF1 and (b) for CF2.

CF2:

$$\frac{\rho_C[v_e(\rho_A) - v_e(\rho_B)]}{\rho_B - \rho_A} = v_e(\rho_C) - \frac{q_e(\rho_A) - q_e(\rho_A)}{\rho_A - \rho_B} = c_0. \tag{14}$$

In Eq. (14), it is interesting to find that ρ_C is the geometric average of ρ_A and ρ_B, i.e.,

$$\rho_C = \sqrt{\rho_A\rho_B}.$$

From Eqs. (5)–(14), all parameters of the two systems are only dependent on the sound speed c_0, the free flow velocity v_f, and the jam density ρ_m. Let the dimensionless variables with a bar correspond to the density that is scaled by ρ_m and the velocity by v_f. It is then convenient to examine that all parameters depend only on $\bar{c}_0$. For CF1 and CF2, the dependencies are shown in Fig. 2 by several curves for a wide range of $\bar{c}_0$. The values of the parameters are also given in Table I. Note that the maximal density $\bar{\rho}_B$ is not valid for $\bar{c}_0 \leqslant 0.5$ in CF1 and for $\bar{c}_0 \leqslant 0.3$ in CF2. Compared with the data acquired from field studies (e.g., in [17]), CF2 seems to give a more realistic description, especially for $0.33 < \bar{c}_0 < 0.40$ that suggest these wave speeds approximately range from 11.5 to 16.5 km per h for $v_f = 30$ m/s.

TABLE I. The minimal and maximal densities $\bar{\rho}_A$ and $\bar{\rho}_B$ of a wide cluster as determined by the system of Eqs. (1) and (7) and the system of Eqs. (1) and (8) for a given $\bar{c}_0$, along with the transition density $\bar{\rho}_C$ and traveling wave speed $\bar{a}$. The cells with an asterisk correspond to maximal densities ρ_B that are obviously greater than unity and thus invalid.

	CF1				CF2			
$\bar{c}_0$	$\bar{\rho}_A$	$\bar{\rho}_B$	$\bar{\rho}_C$	$\bar{a}$	$\bar{\rho}_A$	$\bar{\rho}_B$	$\bar{\rho}_C$	$\bar{a}$
0.30	*	*	*	*	0.09714	1.11416	0.32898	−0.08859
0.34	*	*	*	*	0.10693	0.97766	0.32333	−0.11244
0.35	*	*	*	*	0.10931	0.94904	0.32208	−0.11878
0.40	*	*	*	*	0.12084	0.83021	0.31673	−0.15254
0.45	*	*	*	*	0.13183	0.74125	0.31260	−0.18950
0.50	0.14271	1.00616	0.28494	−0.14160	0.14239	0.67244	0.30944	−0.22921
0.55	0.15263	0.81937	0.28481	−0.19111	0.15263	0.61765	0.30703	−0.27123
0.60	0.16228	0.70171	0.28545	−0.24354	0.16263	0.57283	0.30522	−0.31512
0.65	0.17180	0.62097	0.28660	−0.29794	0.17252	0.53521	0.30387	−0.36050

Furthermore, CF2 also allows a wider range of $\bar{c}_0$ for adjustment to empirical data.

D. Remarks on relations between nonviscous and viscous models

It is well-known from the weak solution theory that the system of hyperbolic conservation laws

$$u_t + f(u)_x = 0 \tag{15}$$

are related to the following standard viscosity system:

$$u_t + f(u)_x = [\epsilon(u)u_x]_x. \tag{16}$$

The physical solution of Eq. (15) is the limit solution of Eq. (16) when $\epsilon(u) \to 0$, where $\epsilon(u)$ is positive and bounded. With an extra relaxation term, we can establish a similar relation between the PW and KK models. Precisely, it is proper to write Eq. (2) of the KK model in the same conservation form as Eq. (8) with a viscosity term μv_{xx} on the right-hand side, i.e.,

$$\frac{\partial q}{\partial t} + \frac{\partial}{\partial x}(q^2/\rho + c_0^2\rho) = \frac{q_e(\rho) - q}{\tau} + \mu v_{xx}.$$

Through this relation, the solution of the KK model is asymptotic to that of the PW model for small μ, corresponding to CF2. This suggests that the KK model cannot be written in the same conservation form as Eq. (7), which corresponds to the PW model in CF1. Otherwise, the resultant viscosity term $(\mu/\rho)v_{xx}$ would be neither bounded nor standard in comparison to Eq. (16). This also implies that the coefficient μ/ρ can never vanish regardless of how small the value of μ is, if ρ is close to zero.

As evidence of the above argument, Kerner *et al.* [11] acquired in their model the same equations as those of Eq. (14) for solving a wide cluster. By these equations, the parameters of the cluster are approximate to the true values (of the KK model) with the error $O(\mu)$, whereas they are exact for the PW model in CF2. This attainment is consistent with the aforementioned relation as the viscosity coefficient μ (precisely the term μv_{xx}) vanishes.

The Kühne model can similarly be written in the same conservation form as Eq. (7) with a viscosity term νv_{xx} on the right-hand side, i.e.,

$$\frac{\partial v}{\partial t} + \frac{\partial}{\partial x}(0.5v^2 + c_0^2 \ln \rho) = \frac{v_e(\rho) - v}{\tau} + \nu v_{xx}.$$

According to the above discussion, it is clear that the Kühne model makes sense through the above relation, and that its solution is asymptotic to that of the PW model in CF1 for small positive constant ν. Applying the asymptotic theory to the Kühne model for solving a wide cluster, as proposed in [11], we anticipate the same equations as those of Eq. (14) and the error $O(\nu)$ of the resultant parameters. This argument implies that it is inappropriate to write the Kühne model in the same conservation form as Eq. (8), which corresponds to the PW model in CF2. In addition, we note that this inappropriate relation would otherwise suggest a viscosity term $\rho\nu u_{xx}$, which is not standard when comparing to that of Eq. (16).

Finally, we note that conservative schemes should be applied for numerical simulations according to the defined or required conservation forms. See such a conservative scheme in Sec. III B.

III. PARAMETERS ACQUIRED FROM NUMERICAL SIMULATION

The instability of the PW model was investigated in Whitham [3] and later in other studies. The linearization of the model equations of Eqs. (1) and (2) results in the following wave equation [3,24]:

$$\xi_t + \lambda_0\xi_x = \tau(\lambda_2 - \lambda_0)(\lambda_0 - \lambda_1)\xi_{xx}, \tag{17}$$

where ξ is the perturbation to the equilibrium flow $[\rho_0, q_e(\rho_0)]$, $\lambda_0 = q_e'(\rho_0)$ is the kinetic wave speed, and $\lambda_{1,2} = v_e(\rho_0) \mp c_0$ are the two characteristic speeds at $[\rho_0, q_e(\rho_0)]$. The viscosity term of Eq. (17) indicates that the equilibrium state $[\rho_0, q_e(\rho_0)]$ is linearly stable if and only if

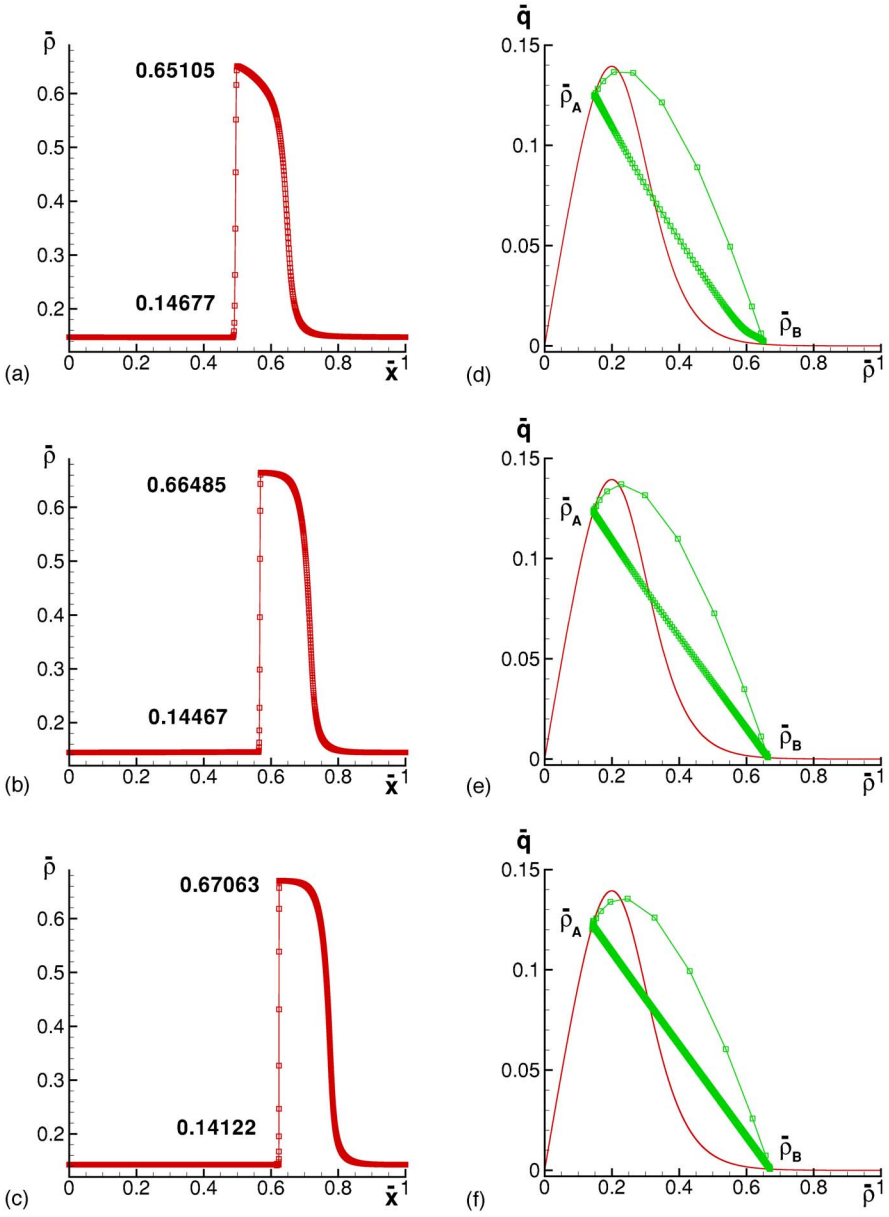

FIG. 3. (Color online) Fully evolved clusters at $t=2500$ s, by CF2 with $\bar{c}_0=0.5$, $\bar{\rho}=0.22$, $\Delta\bar{\rho}_0=0.04$, and $\tau=8$ s. The densities $\bar{\rho}_A$ and $\bar{\rho}_B$ are convergent to those in Table I with the refinement of grids. (a)–(c) Distribution of density $\bar{\rho}$ and (d)–(f) Density-flow states $(\bar{\rho},\bar{q})$ in comparison with the fundamental diagram $\bar{q}=\bar{q}_e(\bar{\rho})$.

$$\lambda_1 \leqslant \lambda_0 \leqslant \lambda_2. \tag{18}$$

For a nonconvex function $q_e(\rho)$, as the one that is given by Eq. (3), there are two critical densities, ρ_{c_1} and ρ_{c_2}, such that the constant state $[\rho_0, q_e(\rho_0)]$ is unstable for $\rho_{c_1}<\rho_0<\rho_{c_2}$, but stable elsewhere [24,26]. For the dimensionless variables, $\bar{\rho}_{c_1}$ and $\bar{\rho}_{c_2}$ depend only on the sound speed $\bar{c}_0$, and the two curves for this dependency are also shown in Fig. 2. We note that $[\rho_{c_1},\rho_{c_2}]\subset[\rho_A,\rho_B]$, and thus the free and jam traffic states A and B of the traveling wave solution are stable.

For the KK model, very close stability conditions for an equilibrium state were derived in [10].

A. Interpretation of the dynamics

The formation of clusters is related to stability conditions. Applying the initial conditions in [10]:

$$\rho(x,0)=\rho_0+\Delta\rho_0\left\{\cosh^{-2}\left[\frac{160}{L}\left(x-\frac{7L}{16}\right)\right]-\frac{1}{4}\cosh^{-2}\left[\frac{40}{L}\left(x-\frac{15L}{32}\right)\right]\right\},\quad v(x,0)=v_e[\rho(x,0)], \tag{19}$$

where the last term in the first equality represents the perturbation to the equilibrium flow $[\rho_0, q_e(\rho_0)]$, and $[0,L]$ is the highway section under consideration. Furthermore, we assume the following periodic boundary conditions:

$$\rho(0,t)=\rho(L,t),\quad v(0,t)=v(L,t), \tag{20}$$

by which the highway is viewed as a ring. Stop-and-go waves can then be induced for $\rho_0\in(\rho_{c_1},\rho_{c_2})$, and the traffic will eventually evolve into regular clusters with free flows in the surrounding as long as $t\to\infty$. Here, the initial conditions

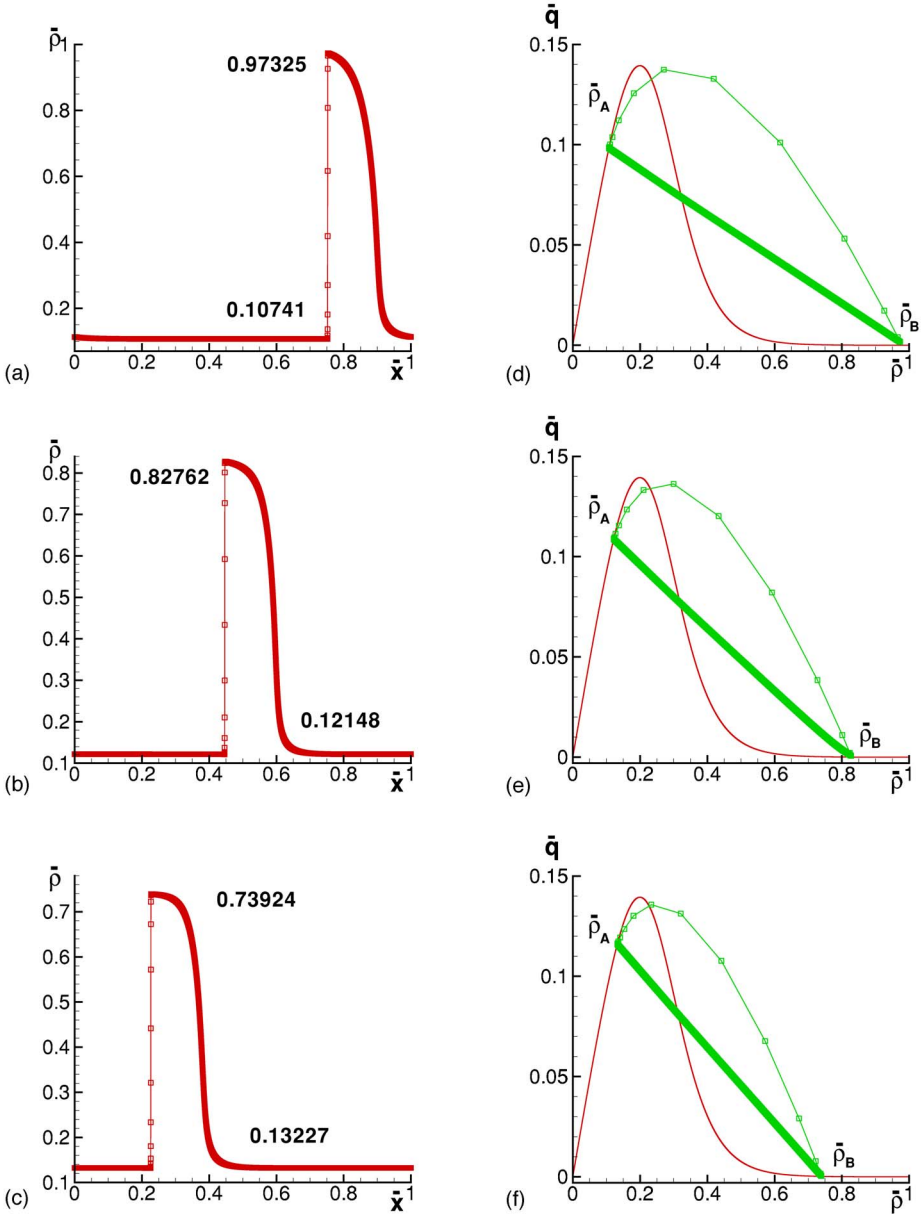

FIG. 4. (Color online) Fully evolved clusters at $t=2000$ s, by CF2 with $N=10\,000$, $\bar{\rho}=0.22$, and $\Delta\bar{\rho}_0=0.04$. (a)–(c) Distribution of density and (d)–(f) density-flow states and the fundamental diagram.

of Eq. (19) suggest that the number of vehicles is $L\rho_0$, which remains unchanged in the ring for the evolution. Numerical examples of this were widely reported, such as in [10,15], and some were given by other higher-order models [23,14].

The formation of the regular clusters are mostly due to the blow-up of an oscillation, or the interaction of irregular oscillations that collide with one another in the ring because they differ in their propagation speeds. These flow states of irregular oscillations (driving behavior) are unstable to remain in or relax to equilibrium. Therefore they must develop or merge into regular clusters which are stable solutions according to the discussion in Sec. II. As evidence of this, equilibrium states A and B are always out of the instability region (Fig. 2). On the other hand, no equilibrium states in the transition layer can be found except for a single state $\rho=\rho_c$, the behavior of which is essentially different from other equilibria because the factor $\rho-\rho_C$ of $q_e(\rho)-q$ is removed [see the discussion for Eq. (5)]. This occurs because most equilibrium states in this density region are not stable. In addition, by the perturbation in Eq. (19), the evolution of the unstable constant solution $\rho=\rho_0$ into the stable traveling wave solution is typical of a metastable physical system.

In the following section, we implement numerical simulation but are mostly interested in these fully developed clusters (at large time t) in the PW model. One can use the same code to generate numerical results at any time to observe the aforementioned chaotic traffic flow.

B. Comparison between numerical and analytical parameter values

We choose ρ_0 in Eq. (19) to be sufficiently large and in the unstable range (ρ_{c_1},ρ_{c_2}). One or more wide cluster [or cluster(s) very close] is then expected. In general, initial conditions with similar density magnitudes of the integral average over $[0,L]$ can also sustain the evolution of the wide

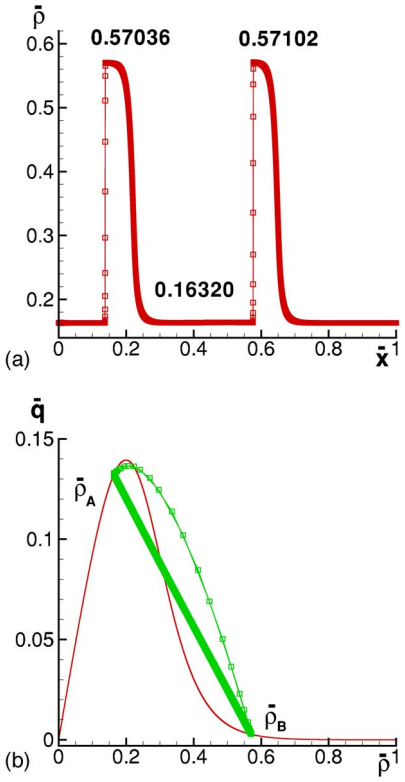

FIG. 5. (Color online) Fully evolved clusters at $t=1500$ s, by CF2 with $\bar{c}_0=0.60$, $N=10\,000$, $\tau=4$ s; the initial conditions are given by Eq. (22) with $\bar{\rho}^-=0.23$ and $\bar{\rho}^+=0.22$. (a) Distribution of density and (b) density-flow states and the fundamental diagram.

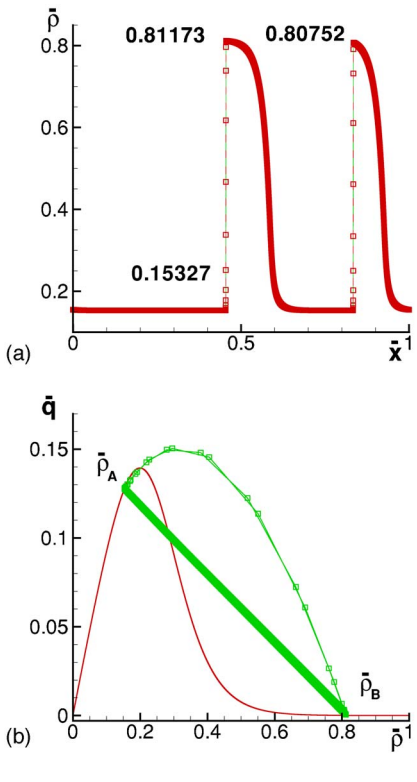

FIG. 6. (Color online) Fully evolved cluster at $t=3000$ s, by CF1 with $\bar{c}_0=0.55$, $N=10\,000$, $\tau=6$ s; the initial conditions are given by Eq. (22) with $\bar{\rho}^-=0.26$ and $\bar{\rho}^+=0.31$. (a) Distribution of density and (b) density-flow states and the fundamental diagram.

cluster(s). In this regard, we note that the periodic boundary conditions are essential for the evolution because they guarantee unchanged integral average density over (or total vehicular number in) the interval. Moreover, they ensure the propagation of these clusters through the boundaries. Through comparison between the analytical and numerical data of the parameters of a wide cluster, we can confirm that the numerical solutions are asymptotical to the described traveling wave solutions.

For this, we apply the first-order Lax-Friedrichs difference scheme

$$u_i^{(n+1)} = u_i^{(n)} - \frac{\Delta t^{(n)}}{\Delta x}(\hat{f}_{i+1/2}^{(n)} - \hat{f}_{i-1/2}^{(n)}) + \Delta t^{(n)} s(u_i^{(n)}), \quad (21)$$

which corresponds to the general system (9). In the scheme, $\hat{f}_{i+1/2}^{(n)}$ is the numerical flux given by

$$\hat{f}_{i+1/2}^{(n)} = \frac{1}{2}[f(u_i^{(n)}) + f(u_{i+1}^{(n)}) - \alpha^{(n)}(u_{i+1}^{(n)} - u_i^{(n)})],$$

$$\alpha^{(n)} = \max_u \max(|\lambda_1|, |\lambda_2|),$$

where $\lambda_{1,2}=v \mp c_0$ are the two characteristic speeds, and the maximum is taken over $u_i^{(n)}$ for all i at time level n. Furthermore, the CFL condition for the numerical stability is taken as

$$\alpha^{(n)} \frac{\Delta t^{(n)}}{\Delta x} = 1.$$

The Godunov scheme appears to be a good choice. However, this is very costly because the application of the exact Riemann solver is implicit and thus considerable iterations are needed. For convenience of illustration and comparison, the dimensionless variables $\bar{\rho}$, $\bar{q}=q/(\rho_m v_f)$, and $\bar{x}=x/L$ are applied in all figures, with $v_f=30$ m/s and $L=10\,000$ m, and the value of ρ_m is unnecessary.

Figure 3 shows the numerical results with all quantities needed in the caption or above the figures. The resultant parameters, namely the values of maximal and minimal densities, are shown in the figures. As the grid is refined, ρ_A and ρ_B [Figs. 3(a)–3(c)] become closer to those that are listed in Table I. We can also observe from the positions of the cluster that the backward-moving wave is slightly slower (from the left to the right). In Figs. 3(d)–3(f), the phase plots are shown on the fundamental diagram $q=q_e(\rho)$ for easy comparison. We can see that (with the refinement) the acceleration path of the transition layer moves closer to a segment from ρ_B to ρ_A, as is indicated in Fig. 1(b). Note that the braking across the upstream front is now replaced by the upper curve that follows the path from ρ_A to ρ_B. This is due to the numerical viscosity that inevitably smooths the shock profile in all numerical schemes. In a similar way, Fig. 4 shows the resultant clusters for several choices of the sound speed $\bar{c}_0$, all of which have the same large grid number N and are very close to those that are listed in Table I.

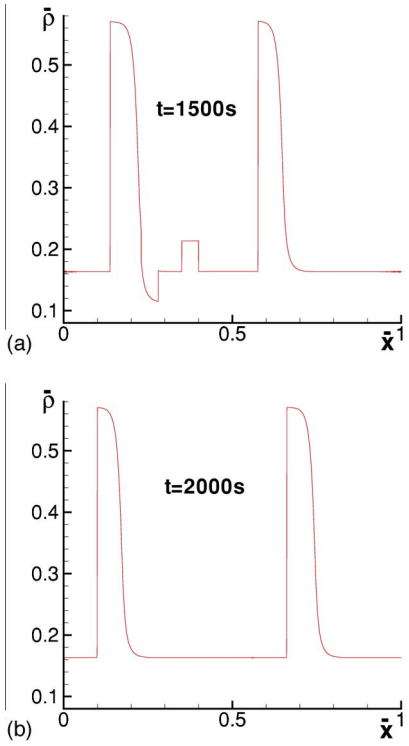

FIG. 7. (Color online) Stability test of fully developed clusters. (a) A perturbed density profile of Fig. 5(a) at $t=1500$ s and (b) recovery of the regular clusters at $t=2000$ s.

Through the above examples (Fig. 3 in particular), we note that numerical results with large grid lengths considerably cut off the upper profile of the cluster due to the resultant numerical viscosity that increases with the grid length. Therefore the resultant maximal density is smaller than that of the analytical result. According to our numerical tests, this can hardly be improved even when well-known higher-order schemes are applied. However, this problem has not been recognized in many studies, in which no analytical data of characteristic parameters have been attained.

Because the mass (total vehicular number) remains unchanged under the periodic boundary conditions (22), the increase in the initial density ρ_0 or the total mass might be able to generate more clusters. This is simply because a greater "mass" would be in supply to fill with the humps. Similarly, more clusters would be expected if we were to decrease the relaxation time τ, by which the mass inside a cluster reduces. This also seems true if we increase the sound speed $\bar{c}_0$. The conclusions are actually implied in Eq. (4) but not detailed in this study.

We alter the initial conditions to be

$$\rho(x,0) = \bar{\rho}^{-}\rho_m \text{ for } x < 0.5L, \tag{22}$$

$$\rho(x,0) = \bar{\rho}^{+}\rho_m \text{ for } x \geqslant 0.5L; \quad v(x,0) = v_e[\rho(x,0)].$$

With such initial data, two clusters are shown in Figs. 5 and 6. As usual the characteristic parameters ρ_A and ρ_B in these two examples again agree well with their counterparts in Table I.

In accordance with the comments in Sec. II D, we note that the numerical schemes of the Kühne and KK models should also be conservative, which is similar to Eq. (21). These correspond to the PW model in CF1 and CF2, with the discretized terms of νv_{xx} and μv_{xx} on the right-hand sides, respectively. Here, the second derivative v_{xx} can be simply discretized by

$$v_{xx} = \frac{v_{i+1} + v_{i-1} - 2v_i}{\Delta x^2}.$$

When the viscosity coefficients ν and μ are small, our numerical tests show little difference in solutions between the Kühne model and the Payne model in CF1, and between the KK model and the Payne model in CF2. One of these examples is shown in Fig. 6(a), to which the numerical result of the Kühne model is added, with the same parameters and a coefficient $\nu=0.01L$. In the comparison, the result is almost identical to that of the PW model in CF1.

For a wide cluster solution, the constant states $\rho=\rho_A$ and $\rho=\rho_B$ are verified to be stable (Fig. 2). However, the stability of the cluster structure (namely the transition layer) needs a rigorous proof, which is a subject for future study. In the present paper, we only test such stability numerically through a perturbation on a fully developed wide cluster. All of the results in the examples that are given in this paper are stable. A typical result of these tests is shown in Fig. 7, in which a perturbed profile of Fig. 5(a) is shown in Fig. 7(a), and the recovery of the regular clusters is revealed in Fig. 7(b). We note that the perturbation should not change the total number of vehicles in the ring.

IV. CONCLUSIONS

Through the study of the PW model, we demonstrate that the weak solution theory can be applied to determine the characteristic parameters of a cluster in traffic flow. Precisely, certain conservation form(s) should be defined and therefore the *Rankine-Hugoniot* conditions can be applied to determine a discontinuity. By the theory and with reliable evidence, we establish the relations between the PW model and the Kühne and KK models. Through these relations, we suggest a certain conservation form of a viscous higher-order traffic flow model, which includes a conservative scheme for numerical discretization.

Compared with the asymptotic theory, the weak solution theory is much easier to apply for solving (or disproving) a wide cluster in higher-order traffic flow models. These determined parameter values are exact in a nonviscous model but serve as a good approximation in the corresponding viscous model. More importantly, the careful treatment of the conservation form for the acceleration equation closes the important gap in the development of higher-order traffic flow models in the literature. Without this conservation form, the solution depends very much on the design of numerical schemes, and can be quite arbitrary and may not adequately conform to the physically relevant properties.

The developed methods can be generalized or directly applied to the studies of other higher-order traffic flow models, or equations that take similar forms. Through

such studies, whether a system can guarantee a solution of wide cluster, or whether the model generates realistic characteristic parameters of the cluster can be indicated analytically.

There are two open but interesting questions that are worthy of future studies. The first is the stability of the discussed traveling wave solution (e.g., the transition layer of the downstream front), which needs a rigorous proof. The second is related to an improved higher-order traffic flow model in Helbing [25], which was developed based on the KK model [10]. It is apparent that the weak solution theory can also be applied to this model, by dropping the higher-order viscosity term. However. the study would be somewhat challenging and more complicated because the model is composed of three equations with the velocity variance being taken as a solution variable in addition to the density and velocity variables.

ACKNOWLEDGMENTS

This work was jointly supported by grants from the Hong Kong Research Grants Council of the Hong Kong Special Administrative Region, China (Grant Nos. HKU7031/02E and HKU7187/05E) and the National Natural Science Foundation of China (Grant No. 10532060).

[1] M. J. Lighthill and G. B. Whitham, Proc. R. Soc. London, Ser. A **229**, 317 (1955).
[2] P. I. Richards, Oper. Res. **4**, 42 (1956).
[3] G. B. Whitham, *Linear and Nonlinear Waves* (Wiley, New York, 1974).
[4] D. Helbing, Rev. Mod. Phys. **73**, 1067 (2001).
[5] G. C. K. Wong and S. C. Wong, Transp. Res., Part A: Policy Pract. **36**, 827 (2002).
[6] P. Zhang, R. X. Liu, S. C. Wong, and S. Q. Dai, Eur. J. Appl. Math. (to be published).
[7] P. Zhang, S. C. Wong, and C. W. Shu, J. Comput. Phys. **212**, 739 (2006).
[8] H. J. Payne, in *Mathematical Models of Public Systems, Simulation Council Proc., La Jola*, 1, edited by A. G. Bekey (1971), pp. 51–61.
[9] R. D. Kühne, in *Proc. 9th Int. Symp. on Transp. and Traffic Theory*, edited by J. Volmuller and R. Hamerslag (VNU Science Press, Utrecht, 1984), pp. 21–42.
[10] B. S. Kerner and P. Konhäuser, Phys. Rev. E **50**, 54 (1994).
[11] B. S. Kerner, S. L. Klenov, and P. Konhäuser, Phys. Rev. E **56**, 4200 (1997).
[12] H. M. Zhang, Transp. Res., Part B: Methodol. **32**, 485 (1998).
[13] S. Rosswog and P. Wagner, Phys. Rev. E **65**, 036106 (2002).
[14] P. Zhang, R. X. Liu, and S. C. Wong, Phys. Rev. E **71**, 056704 (2005).
[15] W. L. Jin, H. M. Zhang, Transp. Res., Part B: Methodol. **37**, 207 (2003).
[16] D. Helbing, Phys. Rev. E **55**, R25 (1997).
[17] M. Schonhof and D. Helbing, e-print cond-mat/0408138.
[18] P. D. Lax, in *Contributions to Nonlinear Functional Analysis*, edited by E. H. Zarantonello (Academic Press, New York, 1971).
[19] P. D. Lax, *Hyperbolic Systems of Conservation Laws and the Mathematical Theory of Shock Waves* (SIAM, Philadelphia, 1973).
[20] J. Smoller, *Shock Waves and Reaction-Diffusion Equations* (Springer-Verlag, New York, 1983).
[21] R. J. LeVeque, *Finite Volume Methods for Hyperbolic Systems* (Cambridge University Press, New York, 2002).
[22] P. Zhang, S. C. Wong, and S. Q. Dai, Chin. Phys. Lett. **23**, 516 (2006).
[23] R. Jiang, Q. S. Wu, and Z. J. Zhu, Transp. Res., Part B: Methodol. **36**, 405 (2002).
[24] H. M. Zhang, Transp. Res., Part B: Methodol. **33**, 399 (1999).
[25] D. Helbing, Phys. Rev. E **51**, 3164 (1995).
[26] T. Li, Commun. Math. Sci. **3**, 101 (2005).